Numerical investigations of drilling mud flow characteristics in vertical well

Nawaf H. Saeid and Bashir S. Busahmin
Flow Modeling and Simulation Research Cluster,
Universiti Teknologi Brunei,
Tungku Link, Gadong, BE 1410, Brunei Darussalam

***Abstract*— Numerical investigations are performed for 3D steady incompressible laminar flow of a non-Newtonian fluid flow in the drilling model in a vertical well. The flow characteristics of the drilling fluid (mud) are presented inside the drilling string including drilling bit and the annulus space under different operating conditions. The composition of a non-Newtonian fluid (mud) is modeled as an aqueous solution of sodium carbomethyl cellulose CMC, a weakly elastic shear-thinning polymer. Parametric study is carried out to optimise the geometry and the operating conditions on the pressure drop of the mud flow from the inlet to the outlet of the well. The parameters considered in the present investigations are: the eccentricity between the drilling string and the casing, the number of the jet nozzles in the drilling bit and the rotational speeds of the drilling string. The present investigation is limited only to laminar flow with Reynolds number at the range $100 \leq Re \leq 1150$. It was found that the pressure drop is reduced by increasing the number of jets in the drilling bit and/or increasing the rotational speed. The results showed that the pressure drop can be increased with an increasing in the dimensionless eccentricity when reaches a maximum at intermediate eccentricity and then decreased with further increase in the dimensionless eccentricity. The results also indicated that the pressure drop is increasing with an increase of the Reynolds number.**

Keywords- Numerical study, Non-Newtonian fluid, drilling mud, eccentric annulus, drilling bit nozzles, Industrial Fluid Mechanics

Nomenclature

D	diameter, m
d_h	hydraulic diameter $(D_o - D_i)$, m
e	distance between the centres of the inner and outer pipes, m
$\vec{g}$	gravity acceleration, ms^{-2}
N	angular velocity, rpm
p	pressure, Nm^{-2}
R	radius, m
r	distance from the inner wall, m
Re	Reynolds number, $Re = U_b d_h/\nu$
S	gap between the inner and outer wall, m
U_b	bulk velocity (volume flow rate/flow area), ms^{-1}
$\vec{V}$	velocity vector, ms^{-1}
x, y, z	Cartesian coordinates, m

Greek Symbols

ε	dimensionless eccentricity, $\varepsilon = e/(R_o - R_i)$
μ	dynamic viscosity, $kg.m^{-1}s^{-1}$
ρ	density, kgm^{-3}
$\bar{\bar{\tau}}$	viscous stress tensor, Nm^{-2}
τ	shear stress, Nm^{-2}
γ	shear rate, s^{-1}

Subscripts

b	bulk
i	inner cylinder
o	outer cylinder

I. INTRODUCTION

In the present study, the mud flow characteristics were investigated numerically during the drilling phase of a vertical well. In any drilling operations, mud is pumped starting from the main tank, through stand pipe pressure, down the drilling string through jet nozzles and back to the surface. The drilling bit that is located at the bottom of the drilling string is designed to have jets to facilitate all drilling operations. The drilling fluid, (mud) along the rock cuttings transfer from the bottom of the hole to the surface with the help of the physical properties of mud and transport velocity, via the annular space that is formed between the drilling string/open hole and casings. In most of straight, vertical and/or directional drilling, the rotating drilling string and the stationary casings always form an eccentric annulus. In reality, this eccentricity varies with depth and mud rheology is always follows a non-Newtonian fluid behavior, due to the contamination of rock cuttings along the formation fluids that includes oil, gas and water [1] (Alderman et al., 1988).

In real time drilling, mud properties in any type of wells rather are complex with numerous parameters. However, a simplified model is shown as a pre-requisite to understand these complex flow behaviors. Understanding the details such as, velocity and pressure variations are so critical for the design and pressure maintenance of the well at various conditions. A review of cuttings transport and approach for monitoring and controlling hole cleaning in directional wellbores is presented

by Nazari et al. (2010) [2]. The review highlighted the effect of the drilling pipe rotation in removing rock cutting at the narrow side of an eccentric well. The flow through annulus, in general, has attracted the attention of many researchers due to its industrial applications including oil-well drilling. There are many studies reported on both Newtonian and non-Newtonian fluids flow in concentric and eccentric annuli, see for example Nouri and Whitelaw (1994), Escudier et al. (2000, 2002), Hemphill and Ravi (2006) and Vieira Neto et al. (2011) [3–7].

Experimental studies on the flow of Newtonian and non-Newtonian fluids in an eccentric annulus with rotating inner cylinder is carried out by Nouri and Whitelaw (1997) [8]. The experiments were carried out on an annulus with an eccentricity of 0.5, a diameter ratio of 0.5, and an inner cylinder rotation of 300 rpm. They reported that the rotation caused the distributions of the velocities across the annulus become more uniform with large variations in cross-flow mean velocities. The Newtonian and non-Newtonian fluids flow resistance increased by more than 30% with rotation at the low Reynolds number (based on the bulk velocity and hydraulic diameter) and it is negligible at the highest Reynolds numbers. For the case of laminar flow of the polymer solution, they found that the rotation caused a counter-rotating swirl flow along the outer pipe wall. This counter-rotating flow was not observed at higher Reynolds number and Rossby number $(2 \times bulk\ velocity/(angular\ velocity \times inner\ radius))$. Similar experimental investigation is conducted by Woo et al. (2006) [9] to study fully developed laminar flows of Newtonian and non-Newtonian fluids through a concentric annulus with inner cylinder rotation. They found that an increase in the speed of the inner cylinder leads to a higher values of pressure drop and an increase in pressure drop depends on the flow regime. Experimental and numerical study is carried out by Escudier et al. (2002) [10] for fully developed laminar flow of a non-Newtonian liquid through both a concentric and an 80% eccentric annulus with and without inner cylinder rotation. The numerical results are in good quantitative agreement with the experimental data even in situations where viscoelastic effects would be expected to play a major role.

The mathematical model of the transport process of mud flow in the annulus is based on the non-Newtonian viscosity of the mud with standard continuity and momentum equations. Computational fluid dynamics techniques are usually employed to numerically investigate the effects of the operational conditions and the fluid properties on the flow structure details of a well model. Manglick et al. (1999) [11] used the finite differences technique to investigate numerically the pseudoplastic flow behavior in eccentric annuli. The effects of eccentricity and viscosity on the friction factor associated to the flow are reported. The authors found a good agreements in their results compared with the experimental data from the Escudier and Gouldson (1995) [12] and Nouri and Whitelaw (1997) [8]. The flow of a non-Newtonian fluids through the annuli formed by two tubes in concentric of a horizontal system that has been investigated numerically by Pereira et al (2007) [13]. The numerical investigation includes the effects of viscosity, eccentricity and shaft rotation on the velocity profiles and on the hydrodynamic losses. The study concluded that the use of CFD provided a satisfactory generation of flow information and allows the expansion of the research horizons for further investigations in this research area. CFD techniques was used by Mme and Skalle (2012) [14] to determine the effects of the parameters, such as geometry, size and physical properties of mud flow on cuttings transportation in various orientation of the well. They found that the mud rheology plays an essential role in cuttings transport. To achieve optimum results for hole cleaning, the studies recommended to use mud at low plastic viscosity in turbulent flow behaviour.

It has been observed, from the above literature review, that most of the studies were focused only on an individual section of the well. Studies of a complete well profile and effects of the parameters such as drilling bits and jet nozzles are not considered in the open literature. Striving by the lack of such important study, the objective of the current study is to simulate the flow behavior in the drilling operation of a whole well under different operating conditions. Figure 1 shows the schematic diagram and the coordinate system of the three dimensional model of the drilling operation that has small annular space between the drilling string and the casing. The drilling string is rotating with a speed of N rpm whereas the outer casing is stationary. The mud is then pumped through the inlet (bit diameter) generating jets due to the flow through the nozzles and flow out to the cased hole.

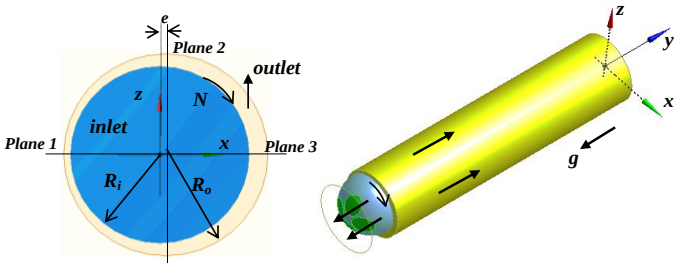

(a) top view (b) computational domain

Figure 1 Schematic diagram of the physical model and the coordinate system

The size of the casing and the drilling string are fixed and adopted from the Halliburton field hand book of standards [15]. The casing diameter is 9.625 inches (= 244.48 mm) or R_o = 122.24 mm. The bit size diameter is 8.5 inches (= 215.9 mm) or R_i = 107.95 mm. However, the dimensionless eccentricity (ε) between the above two cylindrical shapes is considered as one of the parameters under investigation. The diameter of each jet nozzle is 8/32 inches (= 63.5 mm) and is located at 50 mm far from the origin as shown in Figure 1. However, the number of jet nozzles is considered as one of the parameters under investigation. To reduce the computational cost, drilling bit is selected to be y = -1 m.

II. MATHEMATICAL MODEL

The mathematical model and the governing equations of the present problem is based on three-dimensional, laminar and incompressible flow of a non-Newtonian fluid. The governing equations are the continuity and the momentum equations which can be expressed as follows:

$$\nabla.(\rho\,\vec{V}) = 0 \quad (1)$$

$$\nabla.(\rho\,\vec{V}\vec{V}) = -\nabla p + \nabla.\bar{\bar{\tau}} + \rho\vec{g} \quad (2)$$

The stress tensor $\bar{\bar{\tau}}$, is given by:

$$\bar{\bar{\tau}} = \mu\left\{\left(\nabla\vec{V} + \nabla\vec{V}^{T}\right) - \frac{2}{3}\nabla.\vec{V}I\right\} \quad (3)$$

Where $\vec{V}$ is the velocity vector, p is the static pressure, $\vec{g}$ is the gravity acceleration and I is the unit tensor. The fluid properties are: ρ is the fluid density and μ is the molecular viscosity.

The drilling fluid properties reported by Pinho and Whitelaw (1990) [16] is adopted in the current study. The drilling fluid is modeled to be as a 0.2% aqueous solution of CMC which is a non-Newtonian power law fluid flow model with a constant density $\rho = 1000\ kg/m^3$, molecular viscosity at the wall $\mu = 0.0095$ Kg/ms, viscometric power law relating shear stress τ to shear rate to be as γ :

$$\tau = 0.044\,\gamma^{0.75} \quad (4)$$

No-slip boundary condition is imposed on the solid surfaces and constant pressure (atmospheric) boundary condition is imposed at the outlet plan. The mass flow rate is used to identify the inlet boundary condition, whereas the value of the inlet bulk velocity (and therefore the mass flow rate) is calculated from Reynolds number based on the molecular viscosity at the wall and hydraulic diameter.

criteria that follow.

III. NUMERICAL SCHEME

The numerical simulations were performed using ANSYS 14.5 software [17], where the computational domain shown in Figure 1 is generated and meshed. The computational mesh consists of cells generated using the curvature advanced sizing function with medium smoothing and the default setting of the other controls in the global setting in the meshing software of ANSYS14.5 [17].

The cross-sectional of the annular space is meshed using 180 circumferential divisions and 12 divisions in the radial direction as presented in Figure 2(a). Afterthought, 45 uniform size sweep with a quadratic face mesh type is used from the surface (y = 0) to the bottom of the well (y = -1m). At the wellbore, the space surrounding the drilling bit and the jet nozzles is meshed using the triangular face mesh generated automatically using the curvature advanced sizing function [17]. The computational cells were clustered near the jet nozzles, with an element size of 3 mm as shown in Figure 2(b) for the case of drilling bit with 4 jet nozzles.

To ensure an accurate simulation of the sharp gradients of the velocities near the walls, the mesh adjacent to the solid surfaces is made finer than the central region. The total number of elements of the mesh was 516 070 control volumes (cells) for the case of drilling bit with 4 jet nozzles and dimensionless eccentricity of 0.5.

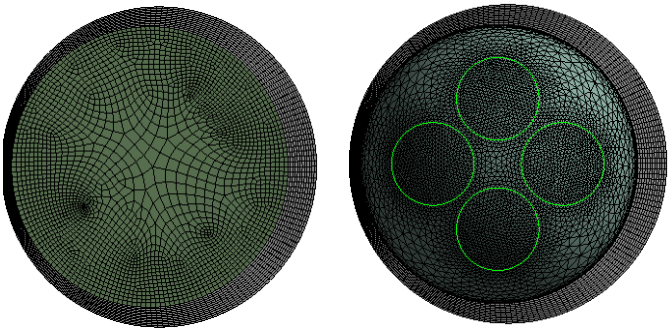

(a) Mesh details at the inlet and outlet. (b) Mesh near the bit nozzles.

Figure 2 Parts of the computational mesh for the case of drilling bit with 4 jets and ε = 0.5

The mesh is then exported to the pressure-based solver build in FLUENT software [18] where the governing equations are solved numerically using the finite volume method. The non-Newtonian power law model defined in equation (4) is used to calculate the drilling mud viscosity. The second order upwind scheme is used for the numerical solution of the momentum equations and PRESTO method, which is recommended [18] for rotating flow, is used for the pressure discretization scheme. The discretized equations were solved based on the pressure correction method with least squares cell based gradient discretisation using SIMPLE algorithm [**19**]. This method is based on the iterative solution and under the relaxation factors of 0.3 and 0.1 which are used for solving the pressure and momentum equations respectively. The convergence criterion is based on the residual in the governing equations. The maximum residual in all of the governing equations were lower than 10^{-3} in the converged solution. The accuracy of the results is then verified utilizing the mass balance. In all of the computational cases the global mass balance are satisfied in the converged solution within a range of $\pm\ 10^{-3}$ %.

IV. RESULTS AND DISCUSSION

The details of velocity and pressure in each control volume at the mesh of the system are generated from the numerical solution of the governing equations. Due to the lack of the experimental data, the flow within the present practical dimensions is compared with an experimental study of Nouri and Whitelaw (1997) [8] of non-Newtonian power law flow in an eccentric annulus. The experimental study of Nouri and

Whitelaw (1997) [8] was focused only on the flow at the annulus and not considered the flow inside the drilling string along the jet nozzles. The results then were validated by comparing the dimensionless velocity profile against dimensionless radial distance of the annular space at the midway along the well (y = -0.5 m). The flow behavior was selected to be laminar with Re = 1150 and the dimensionless eccentricity is $\varepsilon = 0.5$. The current results along with the experimental measurements of Nouri and Whitelaw (1997) [8] at the three circumferential planes are presented in Figure 3. Planes 1 and 3 represent the narrow and the wide gaps respectively, while plane 2 denotes the medium gap at the annular space as depicted in Figure 1(a). Both numerical and experimental results have shown similar trends with a high relative discrepancy at plane 1. One of the more significant reason for this difference in the results is the current used geometry with diameter ratio (D_i/D_o) of 0.883, while the experimental results used a diameter ratio of 0.5. Another reason is related to an overall flow system that is not identical with the experimental setup of Nouri and Whitelaw (1997) [8] as per mentioned above.

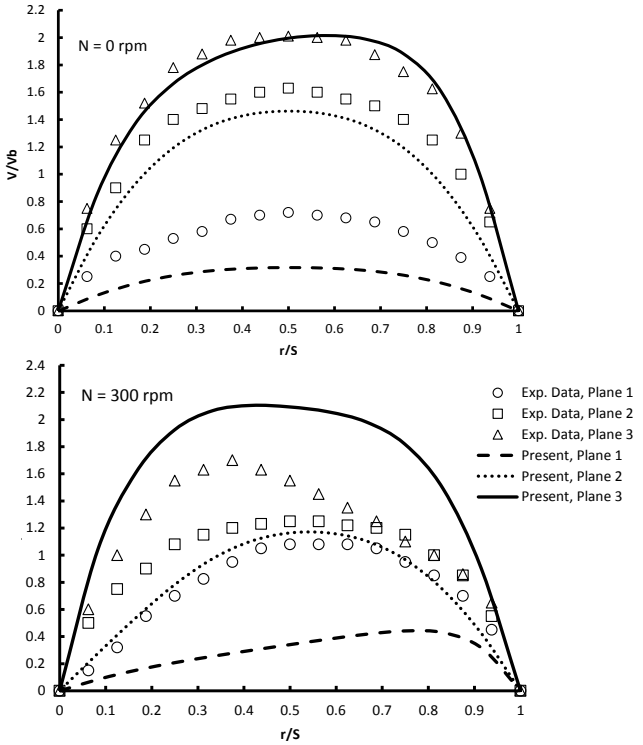

Figure 3 Comparison of numerical and experimental axial velocity profiles at different circumferential planes with ε = 0.5 and Re = 1150 for N = 0 rpm (top) and N = 300 rpm (bottom)

To investigate the effect of the bit depth on the accuracy of the present model, the results were regenerated with an increasing bit depth to 3 m. The velocity profiles showed no significant difference than those presented in Figure 3 at the same conditions, planes and location. Moreover, different mesh sizes were used and the results were generated for each mesh to validate and verify the accuracy of the present simulation method. The mesh with medium size cells defined in the numerical solution procedure was modified to generate meshes with finer and more courser meshes as shown in Table 1. The calculated area-weighted average pressure drops between the inlet and outlet sections are presented also in Table 1. The results show negligible differences in the area-weighted average pressure drops, which indicate the grid independent simulation method. Therefore, the current simulation strategy with the medium mesh size can be considered as valid and will be used to generate the results in the present parametric study.

Table. 1 Pressure drop (Pa) using different mesh size for the case of 4 jet nozzles, Re = 1150 and ε = 0.5.

Total number of cells	N = 0 rpm	N = 300 rpm
363 134 (Big size cells)	649.76459	575.47278
516 070 (Medium size cells)	656.22174	578.76788
919 288 (Small size cells)	660.79169	565.10388

The velocity magnitude vectors and the static pressure contours near the nozzles region are shown in Figure 4 for the case of Re = 1150 and drilling bit with 4 jet nozzles rotating at 200 rpm. To show the flow characteristics through the nozzles, planes passing through the center of the jet nozzles (x = 0 and z = 0) are created as represented in Figures 4(a) and 4(b) respectively. The results indicated that the calculated pressure in the wider gap of the eccentric annulus is higher than that in the narrower gap. The flow circulation can be seen as the mud exits from inside the drilling string, down the bit and up the annulus. In addition, it can be observed from the pressure contours in Figure 4 that there is a negligible pressure drop in the drilling string. However, the pressure contours presented in Figure 4 showed considerable axial pressure drop along the annulus due to the friction between the mud and the annulus surfaces. The high pressure and the high flow velocities near the bottom surface of the well will generate the driving force for the rock cuttings to be transported upwards.

The flow dynamics of the rock cutting is not considered in this study and will be considered in the near future as an extension to the current investigations. Similar flow characteristics are observed in relation to the bit type, such as bits with two and three jet nozzle at various rotational speeds and Reynolds numbers. The axial velocity vectors and the total pressure plots in the midway section (y = 0.5 m) are presented in Figure 5 for different eccentricity using drilling bit with 4 jet nozzles and at a rotary speed of N = 300 rpm and Re = 1150. The velocity vectors at the rotating pipe surface in all cases are presented in Figure 5 show the rotational direction and its effect on the mud flow entrainment in both sides (inside the drilling string, and at the annulus region). The axial velocity values inside the drilling string is relatively small and directed downward, whereas at the annular region the axial velocity directed upward. The axial velocity profiles at the annulus region show parabolic shape at the wider gap and modified at

the narrower gap, because of the effect of the pipe rotation for all the cases as depicted in Figure 5. In all cases, results showed most of the mud mass flow through the wider gap as per (plane 3) of the eccentric annulus due to the low flow resistance as shown in Figures 3, 4 and 5.

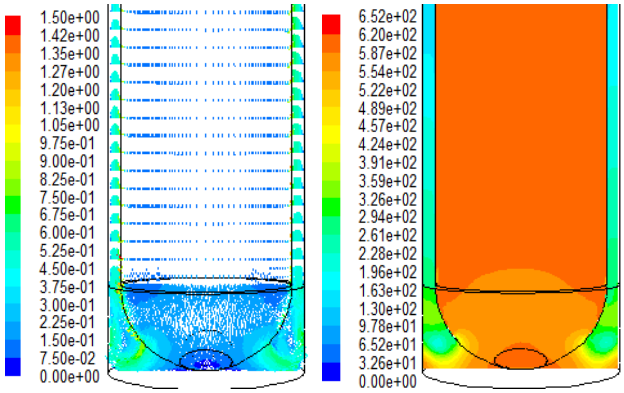

(a) plane x = 0

(b) plane z = 0

Figure 4 velocity magnitude vectors, m/s (left) and static pressure contours, Pa (right) at Re = 1150 using drilling bit with ε = 0.5, 4 nozzles and rotating at 200 rpm

The total pressure drop which is a measure of the driving force for the rock cuttings transport and that is defined as: $p_o = p + \frac{1}{2}\rho\vec{V}^2$. The results are presented in Figure 5 that show the maximum values of the total pressure near the drilling string/pipe wall as a result of the pipe rotation. Afterwards the total pressure is reduced radially towards the center of the pipe from inside and towards the center of the casing from the outer side as shown in Figure 5. The values of the total pressure are high with a large dimensionless eccentricity ($\varepsilon = 0.75$) and then reduced as the dimensionless eccentricity decreases at the same section and rotational speed as shown in Figure5.

To investigate the effects of the governing parameters on the variation of the overall pressure drop, the area-weighted average pressure drop between the inlet and outlet faces is calculated and the results are depicted in Figures 6 and 7. The variation of the pressure drop with the rotational speed is shown in Figure 6 that indicates the pressure drop may be reduced by using more nozzles in the drilling bit and/or higher rotational speed. Similarly, the results presented in Figure 7 shows the pressure drop that maybe reduced by increasing the rotational speed. However the area-weighted average pressure drop from the inlet to the outlet is increasing with an increase of the dimensionless eccentricity when reaches a maximum at $\varepsilon = 0.5$ using a bit size of 4 jet nozzles and Re = 1150.

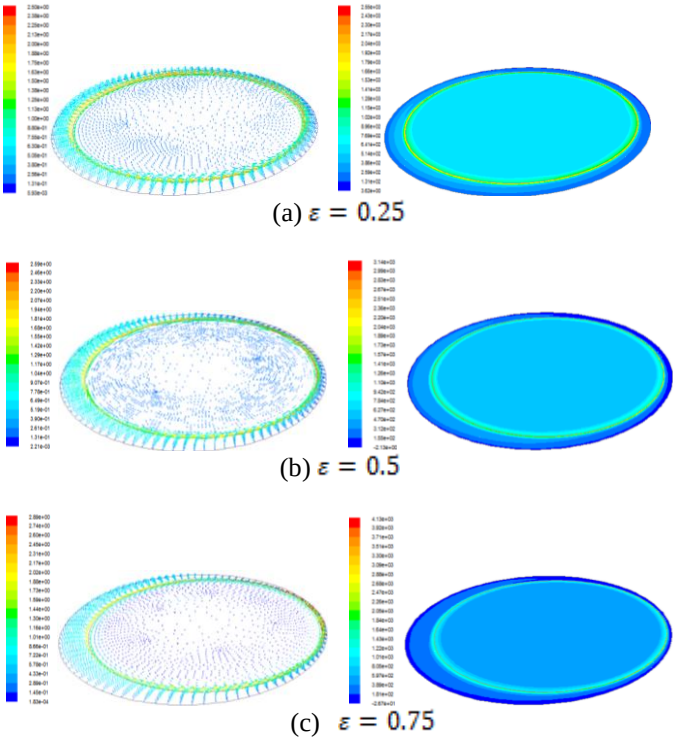

(a) $\varepsilon = 0.25$

(b) $\varepsilon = 0.5$

(c) $\varepsilon = 0.75$

Figure 5 shows axial velocity vectors, m/s (left) and total pressure, Pa (right) in the midway section using drilling bit with 4 jet nozzles and rotating at N = 300 rpm and Re = 1150.

Furthermore an of increase of the dimensionless eccentricity leads to reduce the area-weighted average pressure drop from the inlet to the outlet for the entire rotational speeds as represented in Figure 7. Similar trend is observed by using various bit sizes with different jet nozzles.

The variation of the pressure drop with Reynolds number is shown in Figure 8 for the case of drilling bit with 4 jet nozzles and dimensionless eccentricity of 0.5. The results presented in Figure 8 show that the pressure drop is increasing with an increase of the Reynolds number. In the present analysis, the increase of the Reynolds number is simulated by increasing the mass flow rate of the mud and other parameters remained the same.

The result presented in Figure 8 and Figure 6 showed that the pressure drop is decreased with an increasing the rotational speed of the drilling bit. The results indicate that increasing the pipe rotation leads to reduce the flow resistance and therefore lower pressure needed to pump the mud in the

present system. Similar trend is observed using different number of nozzles with different eccentricities in the drilling bit.

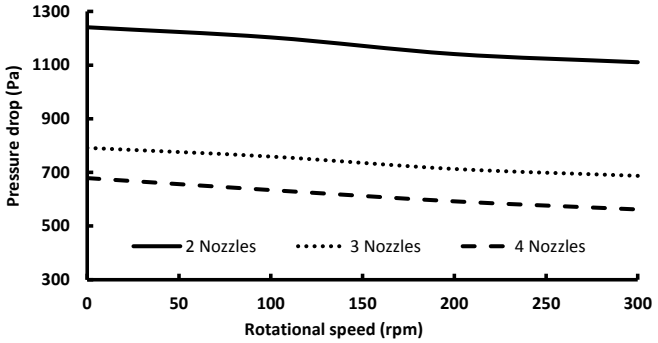

Figure 6 variation of the pressure drop with rotational speed at ε = 0.5 and Re = 1150

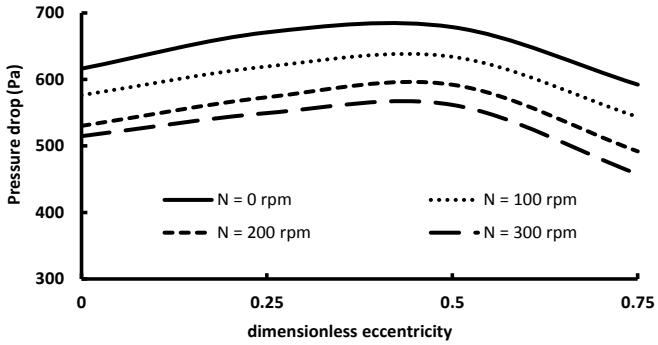

Figure 7 variation of the pressure drop with dimensionless eccentricity using a bit with 4 jet nozzles and Re = 1150

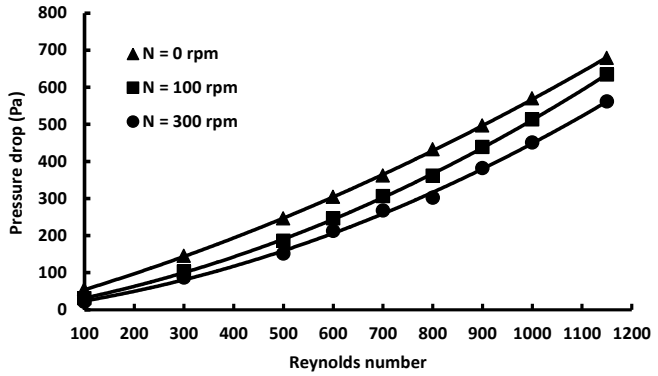

Figure 8 variation of the pressure drop with Reynolds number using drilling bit with 4 jet nozzles and ε = 0.5.

V. CONCLUSIONS

Numerical simulations were carried out in the present study to investigate the characteristics of the 3D steady incompressible non-Newtonian drilling mud flow in a drilling model of a vertical well. The present investigation is limited only to laminar flow with the range of Reynolds number based on the hydraulic diameter of the annular space of $100 \leq \text{Re} \leq 1150$. The composition of mud is modeled as an aqueous solution of sodium carbomethyl cellulose CMC, with power law viscosity model. The flow characteristics details of the drilling fluid (mud) are presented in a complete drilling system, i.e. flow through drilling string, including drilling bit and annular space under different operating conditions. The present study focuses on the investigation of the flow characteristics under different values of the following parameters: (1) the eccentricity between the drilling string and the casing, (2) the number of the nozzles in the drilling bit and (3) the rotational speeds of the drilling string. The results show that most of the mass flow rate of the mud takes place through the wider gap of the eccentric annulus. The results are then presented to show the area-weighted average pressure drop of the drilling mud that flow from inlet to the outlet of the well. It was found that the pressure drop can be reduced by using more nozzles in the drilling bit and/or higher rotational speed. The results also indicated that the pressure drop from the inlet to the outlet is increasing with an increase of the dimensionless eccentricity when reaches a maximum at $\varepsilon = 0.5$ and then was reduced with further increase in the dimensionless eccentricity. In addition the results presented to show the pressure drop increase with an increase of the mass flow rate or Reynolds number.

REFERENCES

[1] N.J. Alderman, D. Ram Babu, T.L. Hughes and G.C. Maitland, "The rheological properties of oil well drilling fluids," Proc. Xth Int. Cong. Rheology, Sydney, pp. 140-142. 1988.

[2] T. Nazari, G. Hareland and J.J. Azar, "Review of Cuttings Transport in Directional Well Drilling: Systematic Approach," paper 132372, Society of Petroleum Engineers, Western Regional Meeting, Anaheim, California, USA, 24-27, May 2010.

[3] J.M. Nouri and J.H. Whitelaw, "Flow of Newtonian and Non-Newtonian fluids in a concentric annulus with rotation of the inner cylinder," J. Fluids Eng., v. 116 (1994) 821–827.

[4] M.P. Escudier, I.W. Gouldson, P.J. Oliveira and F.T. Pinho, "Effects of inner cylinder rotation on laminar flow of a Newtonian fluid through an eccentric annulus," Int. J. Heat and Fluid Flow, v. 21 (2000) 92–103.

[5] M.P. Escudier, P.J. Oliveira and F.T. Pinho, "Fully developed laminar flow of purely viscous non-Newtonian liquids through annuli, including the effects of eccentricity and inner-cylinder rotation," Int. J. Heat and Fluid Flow, v. 23 (2002) 52–73.

[6] T. Hemphill and , K. Ravi, "Pipe rotation and Hole Cleaning in Eccentric Annulus,'' paper SPE 99150 presented at the 2006 IADC/SPE Drilling Conference in Miami, February 21-23.

[7] J.L. Vieira Neto, A.L. Martins, A. Silveira Neto, C.H. Ataide and M.A.S. Barrozo, "CFD applied to turbulent flows in concentric and eccentric annuli with inner shaft rotation," The Canadian Journal of Chemical Engineering. v. 89 (2011) 636–646.

[8] J. M. Nouri and J. H. Whitelaw, "Flow of Newtonian and non-Newtonian fluids in an eccentric annulus with rotation of the inner cylinder," Int. J. Heat and Fluid Flow 18: 236-246, 1997.

[9] N. Woo, Y. Kim and Y. Hwang, "Experimental Study on the Helical Flow in a Concentric Annulus with Rotating Inner Cylinder," Journal of Fluids Engineering Vol.128, 2006, 113-117.

[10] M.P. Escudier, P.J. Oliveira, F.T. Pinho and S. Smith, "Fully developed laminar flow of non-Newtonian liquids through annuli: comparison of numerical calculations with experiments," Experiments in Fluids 33 (2002) 101–111.

[11] R.M. Manglik, P. Fang and M.A. Jog, "Characteristics of laminar viscous shear-thinning fluid flows in eccentric annular channels," Journal of non-Newtonian Fluid Mechanics, v. 84 (1999) 1-17.

[12] M.P. Escudier and I.W. Gouldson, "Concentric annular flow with center body rotation of a Newtonian and a shear-thinning liquid," International Journal of Heat and Fluid Flow, v. 16 (1995) 156-162.

[13] F.A.R. Pereira, M.A.S. Barrozo and C.H., Ataíde, "CFD predictions of drilling fluid velocity and pressure profiles in laminar helical flow," Brazilian Journal of Chemical Engineering, v. 24, No. 04 (2007) 587-595.

[14] U. Mme and P. Skalle, "CFD Calculations of Cuttings Transport through Drilling Annuli at Various Angles," International Journal of Petroleum Science and Technology, Volume 6, Number 2 (2012), pp. 129-141.

[15] Halliburton English/metric cementing tables, Halliburton Company, Duncan, OK 73536, 1981.

[16] F. T. Pinho, and J. H. Whitelaw, "Flow of non-Newtonian fluids in a pipe," J. Non-Newtonian Fluid Mech., 34, 129-144, 1990.

[17] Modeling and Meshing guide, ANSYS, Inc., Southpointe, 275 Technology Derive, Canonsburg, PA 15317, (2009).

[18] FLUENT 6.3 User's Guide, Fluent Inc., Centerra Resource Park, 10 Cavendish Court, Lebanon, NH 03766, (2006).

[19] S.V. Patankar, "*Numerical Heat Transfer and Fluid Flow*," McGraw-Hill, New York, (1980).

AUTHORS PROFILE

Nawaf H. Saeid is a Professor of Thermofluid Engineering at the Universiti Teknologi Brunei (UTB). He received his B.Sc. and M.Sc. degrees from the University of Mosul in Iraq, and his Ph.D. degree from the University Politehnica Bucharest in Romania. He is an academic with wide experience and strong technical and theoretical background in different areas of Mechanical engineering discipline. Possess strong work ethics in 6 different universities, ensuring high performance standards in teaching, research and university administration. His research contribution and expertise include: Thermodynamics, Computational Fluid Dynamics and Heat Transfer, Refrigeration and Air Conditioning, Thermal Energy Management, Acoustics and Noise control, Numerical Techniques and Computer Programming.

Bashir S. Busahmin obtained his higher education from the University of Science & technology from Cracow-Poland and the university of Calgary-Canada both in petroleum engineering, technical drilling engineering and reservoir engineering. Dr. Bashir had worked for Repsol oil operations, as a senior drilling engineer, drilling supervisor as to follow up the drilling operations and activities in the field, and assistant to drilling & workover superintendent for many years. Currently I am working as a principal lecturer at Universiti Teknologi Brunei (UTB) in petroleum engineering, where I am involved in teaching various petroleum engineering courses, such as introduction to petroleum industry, petrophysics, petroleum geology, production geology and geophysics, etc.